



OPEN

Evaluation of fluorescence-based viability stains in cells dissociated from scleractinian coral *Pocillopora damicornis*

Liza M. Roger^{1,2}✉, Yaa Adarkwa Darko¹, Tytus Bernas³, Frances White³, Monsurat Olaosebikan⁴, Lenore Cowen⁴, Judith Klein-Seetharaman^{2,5} & Nastassja A. Lewinski¹✉

The application of established cell viability assays such as the commonly used trypan blue staining method to coral cells is not straightforward due to different culture parameters and different cellular features specific to mammalian cells compared to marine invertebrates. Using *Pocillopora damicornis* as a model, we characterized the autofluorescence and tested different fluorescent dye pair combinations to identify alternative viability indicators. The cytotoxicity of different representative molecules, namely small organic molecules, proteins and nanoparticles (NP), was measured after 24 h of exposure using the fluorescent dye pair Hoechst 33342 and SYTOX orange. Our results show that this dye pair can be distinctly measured in the presence of fluorescent proteins plus chlorophyll. *P. damicornis* cells exposed for 24 h to Triton-X100, insulin or titanium dioxide (TiO₂) NPs, respectively, at concentrations ranging from 0.5 to 100 µg/mL, revealed a LC50 of 0.46 µg/mL for Triton-X100, 6.21 µg/mL for TiO₂ NPs and 33.9 µg/mL for insulin. This work presents the approach used to customize dye pairs for membrane integrity-based cell viability assays considering the species- and genotype-specific autofluorescence of scleractinian corals, namely: endogenous fluorescence characterization followed by the selection of dyes that do not overlap with endogenous signals.

Cytotoxicity, the potential to cause cell death, is measured via different endpoints¹. These endpoints can include membrane integrity, mitochondrial function, proliferation, and apoptosis *versus* necrosis. It is important to systematically combine multiple endpoints, such as membrane integrity and cell death mechanism, to gain insight into the potential pathways involved in cellular toxicity. The most common way to measure these endpoints is by using colorimetric or fluorometric assays which involve the addition of an indicator dye. Many indicator dyes have been developed for different endpoints and finding the right type of dye hinges on the cell model system studied, desired throughput, instruments available for analysis, and cost of reagents². Fluorescent indicator dyes (fluorophores) are most commonly used in biochemical and cell-based assays in vertebrate cell culture since fluorescence is more sensitive³ and fluorescence is utilized in many instruments (microscopy, spectroscopy, flow cytometry). Fluorophores used to assess cytotoxicity mostly emit visible light in the blue, green and red color bands. Table 1 includes common fluorophores used to assess membrane integrity and distinguish between live and dead cells when conducting viability assays.

The need for cellular-scale understanding of mechanisms such as symbiosis, calcification, wound healing and bleaching is increasing as reef-building corals (Scleractinia) are more than ever under stress from rising sea surface temperatures, ocean acidification, diseases, pollution and habitat loss⁴. While many studies have focused on colony-scale or polyp-scale dynamics, cellular studies are less common because the scientific community has only reported generating axenic, immortal scleractinian coral cell cultures twice since the early 1990s (see^{5,6}) and concerns remain regarding contamination and cell identification as our knowledge of the coral holobiont grows^{4,7}. The further development of scleractinian coral cell cultures requires quantitative assessment of survivorship

¹Chemical and Life Science Engineering, Virginia Commonwealth University, Richmond, VA, USA. ²School of Molecular Sciences, Arizona State University, Phoenix, AZ, USA. ³Anatomy and Neurobiology, Virginia Commonwealth University, Richmond, VA, USA. ⁴Department of Computer Sciences, Tufts University, Boston, MA, USA. ⁵College of Health Solutions, Arizona State University, Phoenix, USA. ✉email: rogerlm@vcu.edu; nalewinski@vcu.edu

Fluorophore $\lambda_{ex}/\lambda_{em}$ (nm)	FC*	Type	Findings
Hoechst 33258, 352/461 (blue)	40 μ M	Membrane permeable, non-toxic	Does not penetrate the cells well
Hoechst 33342, 361/497 (blue)	40 μ M	Membrane permeable, non-toxic	Bright stain but needs a minimum of 30 min incubation at 25 °C
NucBlue, 360/460 (blue)	NA**	Membrane permeable, non-toxic	Bright stain, Hoechst 33342 is active agent here
Calcein AM blue, 408/450 (blue)	2 μ M	Membrane permeable, non-toxic	Stains but weakly fluorescent
Calcein AM, 496/515 (green)	2 μ M	Membrane permeant	Overlaps with GFP, cannot be deconvolved
Ethidium homodimer, 528/617 (red)	4 μ M	Membrane impermeant	Efficient and visible staining but must be manually deconvolved from chlorophyll spectrum
POPO-3 iodide, 534/570 (orange)	2 μ M	Membrane impermeant, non-toxic	Cannot be deconvolved using the RFP filter cube but laser scanning microscopy will work
SYTOX Red, 540/658 (red)	0.2 μ M	Membrane impermeant, non-toxic	Efficient and visible staining but must be manually deconvolved from chlorophyll spectrum
SYTOX Orange, 547/570 (orange)	0.2 μ M	Membrane impermeant, non-toxic	Efficient and visible staining but can stain contamination if present
BOBO-3 iodide, 570/602 (orange)	2 μ M	Membrane impermeant, non-toxic	Cannot be deconvolved using the RFP filter cube but laser scanning microscopy will work
Propidium iodide, 585/617 (red)	1 μ g/mL	Membrane impermeant, toxic \geq 24 h	Efficient and visible staining but must be manually deconvolved from chlorophyll spectrum

Table 1. Fluorophores tested on coral cells and conclusions. *FC final concentration in cell suspension. **Not specified by vendor.

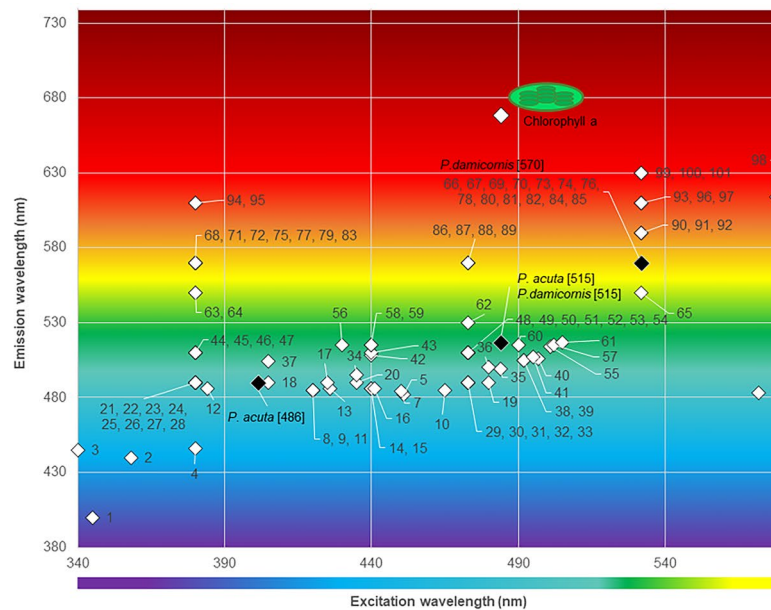
through basic live and dead cell counts. Survivorship being critical to determining culture method success, it is important to have a clear approach for quantifying population viability. The use of trypan blue, a colorimetric, cell impermeant stain, to quantify cell death is the most reported method in relation to coral cell cultures despite its limitations. The main issue with trypan blue is its capacity to bind to proteins in the cell suspension, not just that released by dead cells. This results in blue aggregates that hinder the cell count. There is evidence that trypan blue can be toxic in the case of longer incubation times⁸. Other colorimetric dyes that have been tested on coral cells include cell impermeant stains such as Evans blue and amido black, as well as vital stains such as neutral red and toluidine blue^{9,10}. Nevertheless, the range of imaging and measurement techniques for colorimetric stains are limited in comparison to fluorescent stains⁹. Work on symbiotic algae showed that the nucleic acid stain SYTOX Green (λ_{ex} 504 nm, λ_{em} 523 nm) and propidium iodide successfully labelled nuclei of dead Symbiodinium clade A and B cells⁹ and *Symbiodinium* sp. cells isolated from *Stylophora pistillata*^{11,12}. However, excitation and emission wavelengths of SYTOX Green overlap with green fluorescent protein which is present in many coral host species and certain species of symbiotic algae (e.g. *Breviolum minutum*, formerly Clade B).

Fluorescent proteins extracted from marine invertebrates, especially Cnidarians, have helped advance biological research thanks to their capacity to serve as molecular markers and biosensors¹³. The green fluorescent protein (GFP) was first characterized in the jellyfish *Aurelia victoria* (*Aequorea victoria*)¹⁴ and has now become one of the most useful tools in modern science and medicine¹⁵. Multiple coral chromophores have been identified so far including cyan fluorescent protein (λ_{ex} 404–477 nm, λ_{em} 485–495 nm), green fluorescent protein (λ_{ex} 478–508 nm, λ_{em} 500–520 nm) and red fluorescent protein or symbiotic chlorophyll (λ_{ex} 560–589 nm, λ_{em} 576–595 nm), and non-fluorescent pink-purple-blue (λ_{ex} 560–588 nm)^{16–18} (Fig. 1). Yellow (λ_{ex} 425–550 nm, λ_{em} 525–570 nm) and bright far-red (λ_{ex} 578 nm, λ_{em} 617 nm) fluorescent proteins are also present in corals but appear to be specific to *Agaricia* sp.¹⁹ and *Porites lobata* (pink phenotype)²⁰. It should be noted that, beyond chlorophyll, other endogenous fluorescent signals from the coral microbiome (symbiotic algae included) were not considered here due to the difference in scale at which they might interfere relative to that at which the work was performed. The use of fluorophores in cells with endogenous fluorescent proteins, such as scleractinian coral cells, presents a challenge because fluorophore emission wavelengths can overlap with that of the endogenous fluorescence emitted by fluorescent proteins or symbiotic algae cells (chlorophyll) hosted within coral cells, thereby confounding the signal.

The objective of this study was to tailor a fluorescence-based dye exclusion assay for cell viability and cytotoxicity assessments to scleractinian coral research by taking into consideration the endogenous fluorescent signal (i.e., fluorescent stains to differentiate dead cells from live cells that are detectable in the presence of endogenous cellular fluorescence). To this end we tested established membrane integrity assays developed for vertebrate cells on cells dissociated from *Pocillopora damicornis* (Fig. 2, mixed cells: coral and symbiotic algae) and investigated the overlap between assay fluorophores and endogenous proteins. We then used the resulting protocol to verify the cell viability of dissociated coral cells and test the cytotoxicity of three representative classes of molecules, namely the small molecule Triton X-100, the protein insulin, and a representative engineered nanoparticle, titanium dioxide, as a proof-of-concept and first assessment of the effects of different types of molecules on coral cell physiology.

Results

Tissue of scleractinian coral *Pocillopora damicornis* (green phenotype, Fig. 2) was dissociated from the skeleton using calcium and magnesium-free seawater incubation for 1 h as described in our earlier publication⁴. The mixture of cells was washed and resuspended in complete culture medium (CM, see “Coral cell dissociation and culture” section for details). The resulting cell suspensions were then observed under a confocal laser scanning microscope and analyzed using a fluorimeter to measure the autofluorescence of *P. damicornis*. The



1. <i>Acropora horrida</i>	[400]	42. <i>Pocillopora damicornis</i>	[508]	83. <i>Acropora chesterfieldensis</i>	[570]
2. <i>Pocillopora damicornis</i>	[440]	43. <i>Montastraea cavemose</i>	[510]	84. <i>Acropora chesterfieldensis</i>	[570]
3. <i>Acropora aspera</i>	[445]	44. <i>Acropora divaricate</i>	[510]	85. <i>Favita rotundata</i>	[570]
4. <i>Leptoseris fragilis</i>	[446]	45. <i>Favites complanata</i>	[510]	86. <i>Echinophyllia aspera</i>	[570]
5. <i>Acropora nastura</i>	[482]	46. <i>Acropora chesterfieldensis</i>	[510]	87. <i>Lobophyllia pachysepta</i>	[570]
6. <i>Lobophyllia hemprichii</i>	[483]	47. <i>Favita rotundata</i>	[510]	88. <i>Montipora monasteriata</i>	[570]
7. <i>Acropora secale</i>	[484]	48. <i>Nephtheidae Nephthei</i>	[510]	89. <i>Echinophyllia aspera</i>	[570]
8. <i>Acropora horrida</i>	[485]	49. <i>Montipora turgescens</i>	[510]	90. <i>Cyphastrea microphthalma</i>	[590]
9. <i>Montipora calculata</i>	[485]	50. <i>Hydnophora pilosa</i>	[510]	91. <i>Acropora digitifera</i>	[590]
10. <i>Acropora tenuis</i>	[485]	51. <i>Acropora abrotanoides</i>	[510]	92. <i>Acropora hyacinthus</i>	[590]
11. <i>Porites murrayensis</i>	[485]	52. <i>Lobophyllia hemprichii</i>	[510]	93. <i>Acropora pulchra</i>	[610]
12. <i>Acropora nobilis</i>	[486]	53. <i>Montipora turtlensis</i>	[510]	94. <i>Pocillopora damicornis</i>	[610]
13. <i>Agaricia sp.</i>	[486]	54. <i>Lobophyllia pachysepta</i>	[510]	95. <i>Acropora difitifera</i>	[610]
14. <i>Montastraea faveolata</i>	[486]	55. <i>Montipora monasteriata</i>	[510]	96. <i>Favites complanata</i>	[610]
15. <i>Montastraea cavemosa</i>	[486]	56. <i>Acropora aspera</i>	[514]	97. <i>Stolocoeniella armata</i>	[610]
16. <i>Acropora digitifera</i>	[490]	57. <i>Acropora nastua</i>	[515]	98. <i>Porites lobata</i>	[614]
17. <i>Acropora millepora</i>	[490]	58. <i>Acropora secale</i>	[515]	99. <i>Porites cylindrica</i>	[630]
18. <i>Acropora aspera</i>	[490]	59. <i>Montastraea faveolata</i>	[515]	100. <i>Acropora digitifera</i>	[630]
19. <i>Montipora monasteriata</i>	[490]	60. <i>Montastraea cavemosa</i>	[515]	101. <i>Platygyrus lamellina</i>	[630]
20. <i>Acropora pulchra</i>	[490]	61. <i>Acropora tenuis</i>	[517]		
21. <i>Acropora digitifera</i>	[490]	62. <i>Stylophora pistillata</i>	[530]		
22. <i>Acropora hyacinthus</i>	[490]	63. <i>Porites cylindrica</i>	[550]		
23. <i>Favites ruselli</i>	[490]	64. <i>Acropora dififera</i>	[550]		
24. <i>Platygyrus lamellina</i>	[490]	65. <i>Stolocoeniella armata</i>	[550]		
25. <i>Favites complanata</i>	[490]	66. <i>Porites murrayensis</i>	[570]		
26. <i>Acropora chesterfieldensis</i>	[490]	67. <i>Porites cylindrica</i>	[570]		
27. <i>Favita rotunda</i>	[490]	68. <i>Acropora pulchra</i>	[570]		
28. <i>Neophtheidae Nephthei</i>	[490]	69. <i>Acropora pulchra</i>	[570]		
29. <i>Stylophora pistillata</i>	[490]	70. <i>Montipora digitata</i>	[570]		
30. <i>Montipora turgescens</i>	[490]	71. <i>Porites murrayensis</i>	[570]		
31. <i>Seriatorpora hystrix</i>	[490]	72. <i>Pocillopora damicornis</i>	[570]		
32. <i>Stylophora pistillata</i>	[490]	73. <i>Pocillopora damicornis</i>	[570]		
33. <i>Echinophyllia aspera</i>	[490]	74. <i>Cyphastrea microphthalma</i>	[570]		

Figure 1. 101 Coral chromophores. Selection of 101 coral chromophores excitation (λ_{ex}) and emission (λ_{em}) wavelengths reported in 10 different coral families (43 scleractinian coral species) and measured in *Pocillopora damicornis* (this study). Coral species are listed with number key corresponding to the graph and [emission wavelength] detected (and reported in literature). References are as follow: (1–3, 8–9, 11, 17, 20, 35–36, 38)⁴⁹; (4)⁵⁰; (5, 7, 10, 19, 55–57, 61)⁵¹; (6)⁵²; (12)⁵³; (13)¹⁹; (14–15, 58–59)⁵⁴; (16, 60)⁵⁵; (18, 37)⁵⁶; (21–33, 44–54, 62–97, 99–101)⁵⁷; (39)⁵⁸; (34, 41)¹⁷; (40)¹⁸; (42)⁵⁹; (43)⁶⁰, (98)²⁰.

excitation–emission matrix (EEM, Fig. 3) shows five emission peaks representing tryptophan (λ_{ex} 280 nm, λ_{em} 350 nm, A), cyan fluorescent protein (B), green fluorescent protein (C), red fluorescent protein (D) and the endosymbionts’ chlorophyll (E). The lambda scans confirmed these fluorescent signals (Supplementary Materials S1).

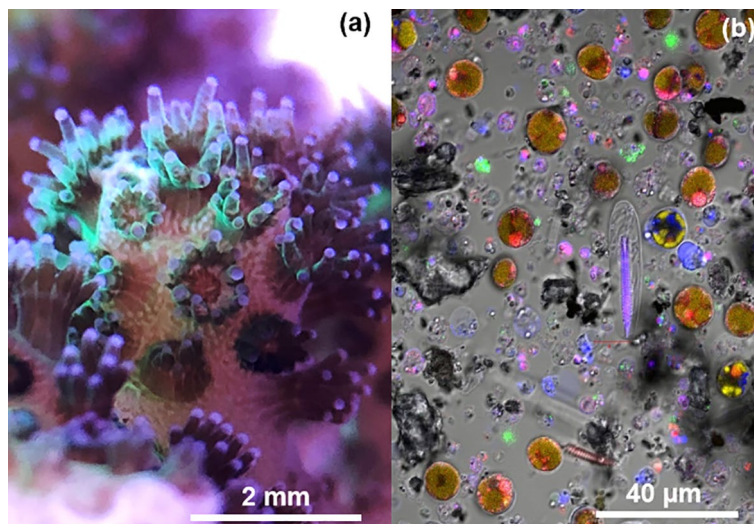


Figure 2. Photograph of *Pocillopora damicornis* in aquarium with polyps displaying the green fluorescent phenotype (a) and cells dissociated from *P. damicornis* stained with ReadyProbes cell viability imaging kit (red: propidium iodide for dead cells, blue: NucBlue for all cells) imaged under confocal laser scanning microscope (Zeiss LSM 710, VCU Microscopy Core) [other colors are as follows: yellow for chlorophyll fluorescence and green for endogenous GFP, DIC set for contrast on center cell] (b). The most recognizable cell types are the symbiotic dinoflagellates (golden-brown rounded cells, color generated from overlay of yellow and red) and the nematocytes (oblong cells with bottle brush-like internal structure). Other cell types cannot be identified from morphological characteristics.

The fluorophores tested on the *P. damicornis* cells were Hoechst 33258 (blue, all cells), Hoechst 33342 (blue, all cells), NucBlue (blue, all cells), Calcein blue AM (blue, live), Calcein AM (green, live), Ethidium homodimer (red, dead), POPO-3 iodide (orange, dead), SYTOX Red (red, dead), SYTOX Orange (orange, dead), BOBO-3 iodide (orange-red, dead), and Propidium iodide (red, dead). The choice of fluorophores to test was guided by emission spectra, staining mechanism and detection capabilities available (confocal laser scanning microscope and microplate reader equipped with the following filter cubes: DAPI, GFP, RFP and Texas Red). Furthermore, a pair of dyes with one indicating dead cells and the other indicating live or all cells was sought for increased accuracy. Calicoblastic cells, i.e. calcifying cells, are $\sim 10\times$ smaller than symbiotic gastrodermal cells and nematocytes (also referred to as cnidocytes, stinging cells) Fig. 2. Without a dye pair combination for viability, cell density can easily be underestimated and smaller cells be inadvertently disregarded as debris. Of these fluorophores, the best combination was Hoechst 33342 and SYTOX Orange with the Hoechst 33342 staining all cells and the SYTOX Orange only the dead cells, leaving the red channel for endosymbiont detection and the green channel for endogenous GFP (Fig. 4, see “Live/dead assay” section for details). The outcomes of staining for all fluorophores tested are summarized in Table 1.

As described in Table 1, several established live/dead stains are ill-suited to coral cells because of spectral overlap with endogenous signals. When using bandpass filters, the emission from the cell impermeant stains propidium iodide and ethidium homodimer cannot be separated from endosymbiont chlorophyll fluorescence to mark dead cells. The nucleic acid stain SYTOX Orange (λ_{ex} 547 nm, λ_{em} 570 nm), also a cell impermeant stain, penetrates cells with compromised plasma membrane and has an emission wavelength further away from that of chlorophyll. The SYTOX line of dead stains is available in different colors, which could be useful in coral samples with emission spectra near 570 nm, as reported for number of Acroporidae, Poritidae, and Faviidae corals (Fig. 1).

Cytotoxicity assay. In order to test the cytotoxicity of titanium dioxide nanoparticles (TiO_2 NPs) and insulin, cell mixtures collected from *P. damicornis* were plated on 96 well-plates coated with poly-D-lysine at a density of $\sim 400,000$ cells per well with complete medium. After a 1 h rest period, the cells were exposed to concentrations of insulin and TiO_2 NPs ranging from 0.5 to 100 $\mu g/mL$ in culture medium. Triton X-100 was used as positive control. Cell survival was measured after 4 h of exposure using the MTS and LDH assays and after 24 h of exposure using the Hoechst 33342—SYTOX Orange dye pair.

Two colorimetric assays were tested here: the MTS and LDH assays. The MTS (3-(4,5-dimethylthiazol-2-yl)-5-(3-carboxymethoxyphenyl)-2-(4-sulfophenyl)-2H-tetrazolium) and LDH (lactate dehydrogenase) assays are commonly performed in combination. Although reliable and simple, limitations of the MTS and LDH assays are that serum and other compounds in the culture media can introduce distortions or background^{21,22}.

The MTS assay did not yield satisfactory results after 1 h at 25 °C, the incubation time recommended for mammalian cells. The expected reaction is a color change from the yellow MTS tetrazolium as it is converted by cell metabolism to the purple/brown formazan. No color change was also measured with longer incubation times of 6, 12, 24 and 48 h at 25 °C. The absorbance measurements of the failed MTS assays are not presented. The LDH assay successfully measured the presence of lactate dehydrogenase in the media taken from the exposed

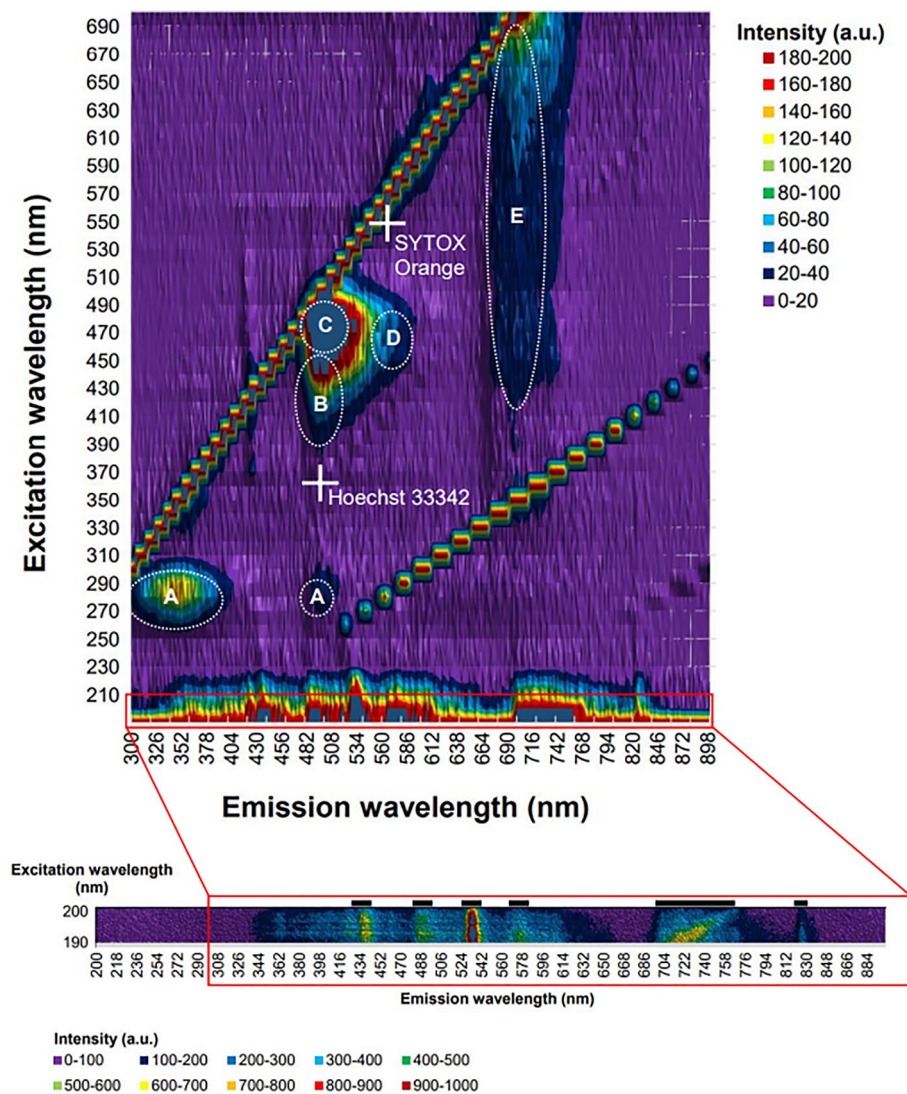


Figure 3. Excitation–emission matrix for *Pocillopora damicornis* from UV/VIS-fluorescence spectrophotometry. Five emission peaks are present: tryptophan (A), cyan fluorescent protein (B), green fluorescent protein (C), red fluorescent protein (D) and chlorophyll (E). Insert shows high resolution fluorescence matrix under deep UV excitation (190 to 200 nm), which also contains the same five emission peaks. Note the chlorophyll fluorescence presents a wide emission band from ~700 nm, which is well documented⁶¹. White crosses represent excitation and emission wavelengths of the dye pair used for membrane integrity assessment (SYTOX Orange and Hoechst 33342).

P. damicornis cell. However, the results were variable and the media-only control was not consistent throughout the experiments (Supplementary Materials S.2).

The measurements based on the Hoechst 33342—SYTOX Orange dye pair showed TiO₂ NPs reduces *P. damicornis* cell viability at concentrations above 10 µg/mL with a calculated lethal concentration 50% (LC₅₀) of 6.21 µg/mL (95% confidence interval, CI from 2.39 to 15.6) after 24 h of exposure. Insulin also reduced *P. damicornis* cell viability (LC₅₀ 33.9 µg/mL, 95% confidence interval, CI from 9.16 to 1736) for concentrations between 10 and 100 µg/mL after 24 h of exposure (Fig. 5). Statistical analysis (two-way ANOVA with blocking and Tukey post-hoc, see “Statistical analysis” section) revealed significant differences between the control (0 µg/mL) and concentrations above 1 µg/mL for all treatment (Supplementary Materials S.2). Significant differences were also found between the positive control treatment (Triton X-100) and TiO₂, and insulin, confirming its efficacy as positive control. No significant difference was found between the TiO₂ and insulin treatments (Fig. 5, Supplementary Materials S.2).

Discussion

Mammalian cell-based assays are poorly adapted to in vitro work with scleractinian coral cells. This is in part due to the diversity and abundance of endogenous fluorescence present in reef-building corals but also due to factors such as the lack of cell attachment, the salinity (~35‰) or strong ionic (~0.7 M) nature of seawater, and

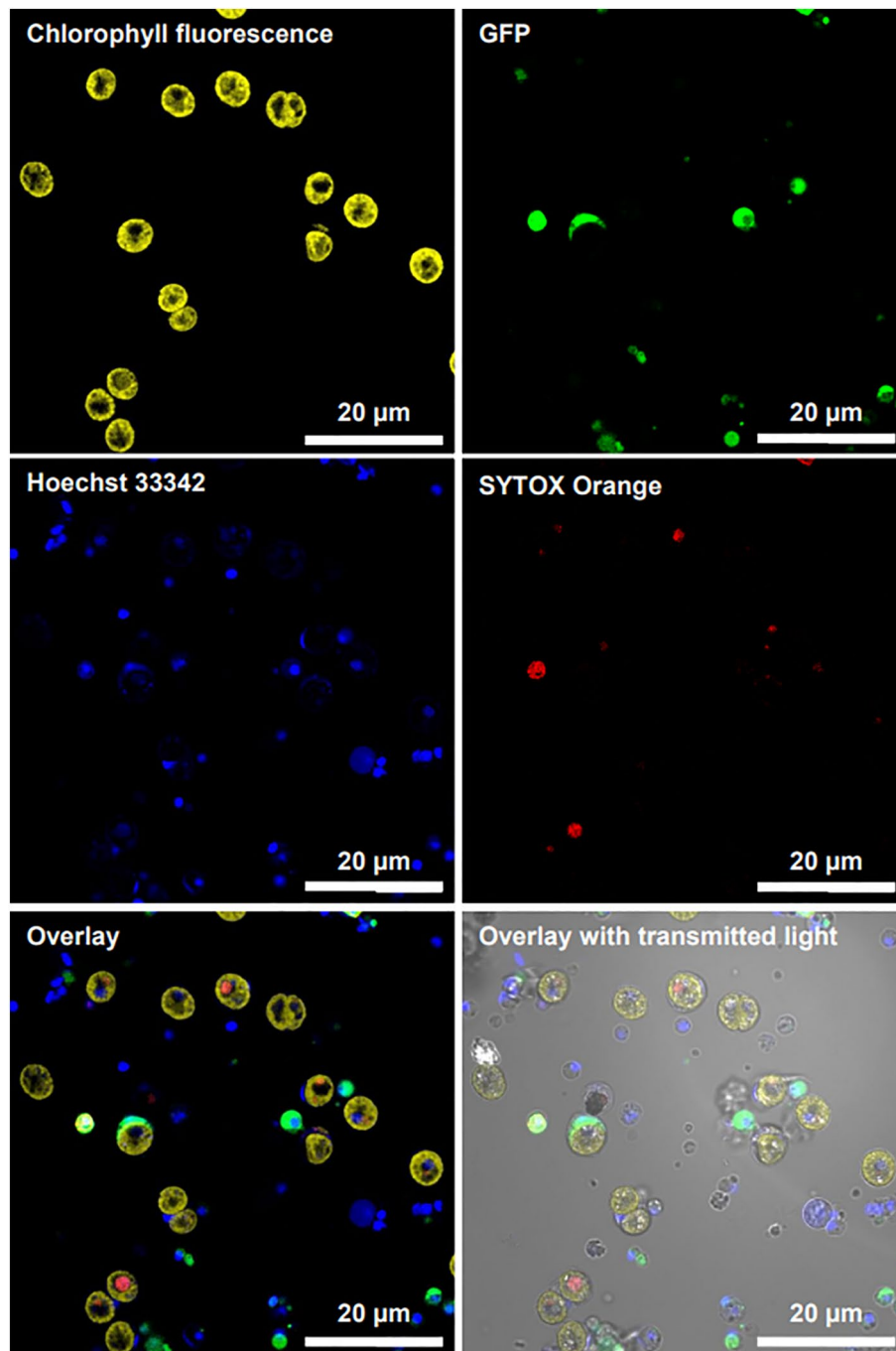


Figure 4. Live cell confocal fluorescence laser scanning microscopy images of *Pocillopora damicornis* cells (Zeiss LSM 710, VCU Nanomaterial Characterization Core). Cells were co-stained with SYTOX Orange (0.2 μ M) and Hoechst 33342 (40 μ M) for 30 min. Magnification = 63 \times .

other unknowns. Indeed, as our knowledge of coral cell physiology and function grows, so will the diversity of coral-specific assays. Coral cell viability assessment is key to developing other assays as cell viability is one of the most straightforward endpoints of in vitro research. In this study we developed a framework for coral scientists to tailor fluorescence-based membrane integrity assays to the coral species phenotype of their choice. This method first involves accurately determining the different fluorescent signals emitted by the coral species genotype and finding fluorescent dyes that do not overlap or that can easily be deconvolved. The membrane integrity-based dye pair Hoechst 33342-SYTOX Orange, avoids the endogenous fluorescent signals of *P. damicornis* cells, allows for determination of cell viability independent of a reference (control) sample, and allowed us to test the toxicity of TiO₂ and insulin in vitro applied to cells dissociated for scleractinian coral *P. damicornis* (green phenotype) for the first time.

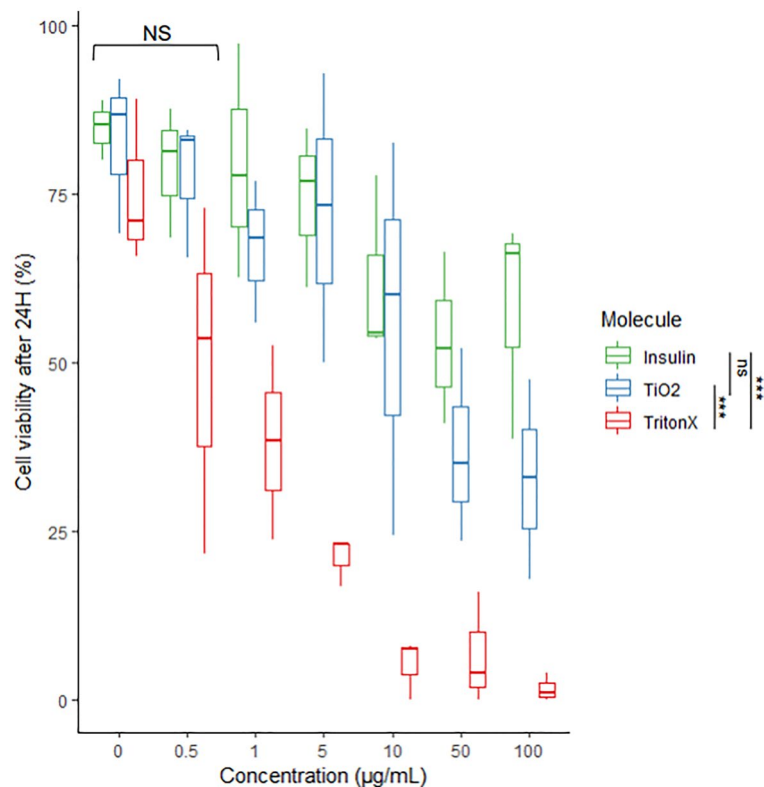


Figure 5. Coral cell viability after 24 h exposure to concentrations of Triton X-100 (positive control, cell lysate), titanium dioxide (TiO_2) and insulin between 0.5 and 100 $\mu\text{g/mL}$. The boxes summarize the data with median (bold line) and outliers (whiskers). The different molecules tested yielded statistically significant results between 1 and 100 $\mu\text{g/mL}$ but not between 0 and 0.5 $\mu\text{g/mL}$ (NS). The control used (Triton X-100) yielded significantly different results compared to TiO_2 and insulin, confirming its role as positive control. Further statistical analyses can be found in Supplementary Materials S.2.

Two viability assays common in mammalian research, the MTS and LDH assays, were also tested yielding unsatisfactory results. Cell viability has previously been tested using the MTT tetrazolium reduction assay²³. Both MTT and MTS are tetrazolium-based dyes; however, MTS relies on an intermediate electron acceptor for reduction to formazan. In addition, the background absorbance from the culture media and MTS alone at the measurement wavelength of 490 nm is higher than the background absorbance for the MTT assay²⁴. The inconsistencies in the LDH assay results on the other hand, might be due to the presence of other dehydrogenases, such as opine dehydrogenases which are functionally analogous to lactate dehydrogenase, being used to regenerate NAD^+ in many invertebrates²⁵. *Montipora capitata*, another scleractinian coral, showed strombine dehydrogenase and alanopine dehydrogenase activity but no LDH activity²⁵. Another potential explanation for the poor results of the LDH assay could be the rich protein content of the complete culture medium (including 5% FBS) used to suspend the cells isolated from the coral fragments. Coral cell viability is reduced in the absence of serum⁴ but an alternative approach could use complete culture medium made with heat inactivated serum²⁶. Because both these assays rely on normalizing the measurements to a reference to quantify cell viability, we did not pursue further optimization of the assays in this study.

One of the complications associated with *in vitro* coral research is limited cell attachment. Compared to adherent mammalian cell lines which attach to the substrate, coral cells have shown limited attachment to standard culture flasks and plates⁴. Here, we worked with mixed, unsorted cells; therefore, we increased cell attachment by coating the well plates with poly-D-lysine to reduce cell loss during aspiration. Without poly-D-lysine, cell counts dropped drastically and reached levels below critical mass. Poly-D-lysine had the side effect of trapping the TiO_2 nanoparticles which resulted in the persistence of TiO_2 agglomerates after exposure medium washing, which is visibly present in the brightfield images. The entrapment of TiO_2 particles could have reduced their interactions with *P. damicornis* cells and affected the measured cytotoxicity. TiO_2 nanoparticles have strong UV photoactive properties which have led to their increased use in paints, solar cells, and sunscreens and consequently their unintentional release in the environment²⁷. The toxicity of TiO_2 particle exposure in various freshwater (reviewed in²⁸) and marine organisms (reviewed in²⁹) has been tested, and the toxicity has been shown to increase with UV exposure due to photoactivation^{28,29}. It is important to note that UV conditions are not always reported making it challenging to determine UV-enhanced cytotoxicity. The light requirements of reef-building corals intrinsically involve UV exposure, and we applied a 10 h light/14 h dark cycle (PAR 40 ± 2 , i.e. $\sim 8.71 \text{ W/m}^2 = 0.0871 \text{ mJ/cm}^2$, see “Materials and methods” section for more details) throughout our

experimentation. TiO₂ particles, with particle sizes ranging from 20 to 200 nm have been shown to damage symbiotic dinoflagellates and induce bleaching in *Acropora* spp. corals³⁰ and *Montastraea faveolata*³¹. In both *Acropora* and *Montastraea*, slight bleaching occurred after exposure to 6.3 mg/L TiO₂ for up to 48 h and 10 mg/L TiO₂ for 17 days. Our results corroborate these findings with a reduction in cell viability starting at 10 mg/L TiO₂ with LC50 at 6.21 mg/L under a UV intensity five times lower than that experienced in the environment. Concentrations of TiO₂ measured in seawater collected in coastal areas were reported to range between 0.02 and 0.9 mg/L of TiO₂ per day based on a study performed along three beaches in the south of France³² and 7–40 µg/mL of TiO₂ along three beaches of Majorca Island³³. These concentrations, which were correlated to sunscreen use by beachgoers, are orders of magnitude less than the LC50 found here; however, studies to date including ours represent only short term exposures.

The symbiotic mutualism between coral host and dinoflagellate endosymbionts fulfills up to 90% of the holobiont's energetic needs. This energy trafficking suggests a transport and signaling system where a molecule such as insulin could come into play. Furthermore, as bleaching involves the breakdown of symbiosis, this transport and signaling system can be disrupted, presumably with similarities to the diabetic response in vertebrates. Insulin production is recognized as an evolutionary ancient function and its presence has been demonstrated in many organisms in addition to humans (unicellular eukaryotes, fungi, worms, fruit flies). There are numerous reports of preproinsulin-like pseudogenes in a variety of different organisms including insects, invertebrates, plants and microbial eukaryotes and prokaryotes³⁴. Remarkably, human insulin has been shown to have physiological effects on other organisms, such as *Acanthamoeba castellanii*³⁵, suggesting a conservation of structure and function across long evolutionary distances. A genome-wide computational scan of *P. damicornis* predicted protein sequences, using Hhblits³⁶ to look for remote homologues of human protein sequences, predicts that *P. damicornis* cells (host coral) have insulin and insulin receptors (see Supplementary Material S.3)³⁷. To enable future investigation of this hypothesis, we investigated insulin cytotoxicity here as an example for proteotoxicity. Insulin has been a model system for the study of proteotoxicity in protein evolution³⁸, and different conformations and oligomerization states of insulin are relevant in the etiology and treatment of diabetes^{39,40}. Thus, the natural first step in evaluating the effects of insulin on *P. damicornis* is its potential cytotoxicity. Our findings suggest that insulin reduces *P. damicornis* cell viability (~18% decrease) at concentrations between 10 and 100 µg/mL. Insulin cytotoxicity is known to depend on different solvent properties, such as increased temperature and high concentrations of salts^{41,42}, leading to insulin aggregates and misfolding. The salinity or the ionic strength of seawater could have had similar effects despite the relatively low temperature (25 °C) and basic nature of the culture medium. Thus, it is possible that seawater might be modifying insulin conformation and cytotoxic behavior, and the present work lays the foundation for further research related to the effects of insulin on corals.

The insulin concentration in the serum used was unfortunately not available however, based on similar products, we estimate the insulin from the FBS used contributed less than 0.04% of the lowest concentration tested (0.5 µg/mL) for cytotoxicity in this study.

Regardless of the organism studied, the type of cell death mechanism is highly dependent on the nature and duration of the stress applied and the ability of cells to maintain homeostasis. The positive control, Triton X-100, is a common surfactant used to lyse cells. It is cytotoxic to a number of cell types: ciliated protozoan, fish and mammalian⁴³. Using it as a positive control for membrane integrity assays involves the understanding that cell count will decrease with increasing Triton X-100 concentration. Different mechanisms of cell death can be involved when coral cells are exposed to substances such as insulin and TiO₂ NPs tested here. Therefore, the Triton X-100 serves as a positive control verifying that the assay worked and additional research is needed to identify the mechanisms of cell death. For example, in mammalian cells, the absence of caspase activation, cytochrome c release, DNA fragmentation, membrane damage and changes in cell morphology are all cell parameters that can be used to discriminate cell necrosis from apoptosis⁴⁴ and other types of cell death. This distinction is also particularly relevant in the study of dysbiosis. The breakdown of symbiosis between endosymbiotic dinoflagellate algae and coral host is still not well understood⁴⁵ despite the urgent need to characterize coral bleaching at the cellular level. Stable cultures of the endosymbiont-holding gastrodermal cells, combined with cytotoxicity and cell death mechanism assays could help better define the mechanisms of coral-dinoflagellate dysbiosis.

Conclusion

The global loss of coral cover driven by anthropogenic climate change has underscored the need for a better understanding of coral cell biology. Research progress in this area will be driven by the optimization of marine invertebrate cell culture methods and the potential transfer of in vitro methods developed for model organisms. Cell viability is a key measurement, and development of membrane integrity assays for coral cell culture represents an essential step in the advancement of in vitro coral research. Our results show that the Hoechst-SYTOX dye pair is well suited for membrane integrity assessments in *P. damicornis* cells. This dye pair was used to measure quantitatively the toxicity of Triton X-100, TiO₂ and insulin in coral cells for the first time in vitro. These results open the door to in-depth, quantitative evaluation of toxicity of different reagents on corals at the cellular level.

In addition, further development of cellular assays will provide new tools to better understand cnidarian cellular physiology, transmembrane exchanges and cell death mechanisms.

Methods

Coral cell dissociation and culture. Fragments of *Pocillopora damicornis* (ORA Aquaculture purchased from Live Aquaria, FL) were maintained in 37.8L aquaria and supplied with oxygenated artificial seawater (ASW, constant bubbling, reverse osmosis deionized water [5 Stage Premium RO/DI water saver system from Bulk Reef Supply] + Fritz Reef Pro Mix salts, SG 1.025 ± 0.002, pH 7.5–8, 25 °C ± 1 °C, pump flow rate: 378.5 L/H, pump

filter: activated carbon Aqueon, 10 h-light/14 h-dark cycle AI Prime 16HD Reef light: blue 28%, royal 28%, green 28%, deep red 28%, UV 28%, violet 28%, cool white 28%, moonlight 28%, PAR 40 ± 2). The spectrum of the AI Prime 16HD light ranges from 380–700 nm with the highest intensity peak wavelength being 450 nm at peak PAR of 100 Mol (<https://www.aquillumination.com/products/prime>). The LED wavelengths are as follows: blue 460–490 nm, royal blue 450 nm, green 520–550 nm, deep red 660 nm, UV 400 nm, violet 415 nm (note: no wavelength available for the moonlight LEDs). General weekly maintenance included tank cleaning to remove macroalgae overgrowth, coral feeding (live Artemia: Carolina brine shrimp eggs) and replacing 2L of seawater.

The cell dissociation protocol follows that reported in Roger et al.⁴ Briefly, a coral nubbin (*P. damicornis*) of ~5 mm length was cut using sterile clippers and placed in artificial seawater (RO/DI H₂O + Fritz Reef Pro Mix) with Reef Dip coral disinfectant (25 μ L/mL of seawater) under constant bubbling for 10 min. The nubbin was then rinsed with sterile filtered (0.22 μ m pore polyethersulfone membrane to remove any potential particulates), autoclaved ASW 3 times and incubated in calcium- and magnesium-free ASW (autoclaved and sterile filtered) for 1 h in a biosafety cabinet under ambient light. The nubbin was then washed using the solution in the vial to detach remaining cells and maximize cell count. The cell suspension was centrifuged at 1200 rpm (204 RCF) for 3 min at 25 °C and the supernatant replaced with complete culture medium (CM). The complete CM is composed of 15% Dulbecco's Modified Eagle Medium (without phenol red, with 17.491 M D-glucose, 2.50 mM L-glutamine) + 5% Fetal Bovine Serum + 0.5% antibiotic-antimycotic + 0.5% gentamicin + 79% filtered sterile ASW.

TiO₂ and insulin exposures. Dissociated coral cells in complete coral CM were plated in poly-D-lysine coated 96 well plates at a density of ~400,000 cells per well. Poly-D-lysine (ThermoFisher cat. No. A3890401) coated 96 well plates were prepared following the manufacturer's protocol. Initial viability was assessed using a 1 mL aliquot of the cell suspension stained with the Hoechst 33342/SYTOX Orange live/dead staining solution and counted on a disposable hemocytometer (INCYTO C-Chip, Neubauer Improved format) prior to plating. Following a 1 h rest period (to allow for potential membrane repair⁴⁶ and attachment to polylysine coated culture substrate⁴⁷), cells were incubated in coral CM alone (negative control) or coral CM containing serial dilutions (0.5, 1, 5, 10, 50 and 100 μ g/mL) of Triton X-100 (positive control, Sigma-Aldrich cat. no. T8787), insulin (human recombinant (yeast), MilliporeSigma cat. no. 11376497001), or TiO₂ nanoparticles (nanopowder, 21 nm primary particle size, $\geq 99.5\%$ trace metals basis, Sigma-Aldrich cat. no. 718467, characterization data presented in Supplementary Materials S.4) for 24 h at 25 °C. Triplicate wells were exposed for each dose and the assay was performed three times. After exposure, the plates were centrifuged at 1200 rpm (204 RCF) for 3 min at 25 °C. The medium was replaced by the Hoechst 33342/SYTOX Orange live/dead staining solution and incubated in the dark for 30–60 min. After staining the plates were centrifuged at 1200 rpm (204 RCF) for 3 min at 25 °C. The staining solution was aspirated and fresh coral CM was added to each well before imaging. Photos of each well (4 \times magnification) were taken using a Cytation3 microplate reader mounted with 4 filter cubes (BioTek Agilent): DAPI (λ_{ex} 350–405 nm, λ_{em} 415–480 nm), GFP (λ_{ex} 445–490 nm, λ_{em} 501–550 nm), RFP (λ_{ex} 505–560 nm, λ_{em} 520–570 nm) and Texas Red (λ_{ex} 575–600 nm, λ_{em} 510–585 nm). Cells were counted in each photo and percent viability post-exposure was determined by [(Hoechst positive cells—SYTOX positive cells)*100/(Hoechst positive cells)]. Cell counting was performed using BioTekGen5 software automation in 1000 \times 1000 μ m squares in each photo (five photos were taken in each well).

Live/dead assay. Two fluorescent dyes were selected: Hoechst 33342 (20 mM, ThermoFisher cat. no. 62249) and SYTOX Orange (250 μ M solution in DMSO, ThermoFisher cat. no. S34861). To a 1 mL coral cell suspension, 10 μ L of SYTOX Orange (0.2 μ M final concentration) and 2 μ L of Hoechst 33342 (40 μ M final concentration) were added. Hoechst 33342 and SYTOX Orange are both DNA-binding dyes; however, Hoechst 33342 is membrane permeable whereas SYTOX Orange is not. In other words, Hoechst 33342 stains all cells while SYTOX Orange stains only cells with damaged membranes. Cells were exposed to the staining solution for 30–60 min and washed with fresh complete coral CM before imaging.

MTS and LDH assays. Dissociated coral cells were plated in 96 well plates at a density of ~250,000 cells per well in complete coral CM. After a 1 h rest period, initial viability was assessed using a small aliquot of the cell suspension stained with the Hoechst 33342/SYTOX Orange live/dead staining solution and counted on a disposable hemocytometer prior to plating. Cells were incubated in coral CM alone (negative control) or coral CM containing serial dilutions (0.5, 1, 5, 10, 50 and 100 μ g/mL) of Triton X-100 (positive control), insulin, or TiO₂ NPs for 4 h at 25 °C. Triplicate wells were exposed for each dose and the assay was performed three times. After exposure, the plates were centrifuged at 1200 rpm (204 RCF) for 3 min at 25 °C. A 50 μ L volume of supernatant from each well was transferred to a white 96-well plate and left to equilibrate to room temperature for 20 min. Then, 50 μ L of CytoTox-ONE reagent (CytoTox-ONE Homogeneous Membrane Integrity Assay kit, Promega, G7891) was added to each well and incubated at room temperature for 10 min. After adding 25 μ L of Stop Solution to each well, the fluorescence intensity was measured at λ_{ex} 560/ λ_{em} 590 nm using a microplate reader (Cytation 3, BioTek).

The remaining exposure medium was removed from the wells and 120 μ L of MTS reagent was added to each well. The MTS reagent consisted of 7.1 mL of coral CM and 1.4 mL of MTS (CellTiter 96 Aqueous One Solution Cell Proliferation Assay kit, Promega, G3580). The plate was incubated at 25 °C for 1 h in the dark. Following incubation, the absorbance was measured at 490 nm using a microplate reader.

Statistical analysis. The cell viability data was analyzed using a two-way ANOVA with blocking to consider variability between replicate assays (viability ~ concentration + assay + molecule), and Tukey post-hoc (95% family-wise confidence level). The LC50 of Triton X-100, TiO₂ NPs and insulin were calculated using the probit

regression model in the R package *ecotox*⁴⁸ v. 1.4.4 available on CRAN. All analyses performed and results can be found in Supplementary Materials S.2.

Microscopy: laser scanning microscopy. Single optical sections of coral cell suspension were acquired with a Zeiss LSM 880 or LSM 710 confocal microscope, build on Axio Observer Z1 inverted stand, equipped with motorized stage and a 40× Plan Apo oil immersion objective (NA 1.4). Fluorescence was excited with either one or a combination of lasers available on the system: 405 nm diode (15 mW), 440 nm diode (15 mW), multiline Ar ion (458/488/514 nm, 25 mW), 561 nm DPSS (15 mW), 594 nm and 633 nm He–Ne (3 mW each). Excitation power was adjusted between 0.8% and 2%, depending on the line. Fluorescence spectrum was registered with a 32-channel spectral hybrid detector at the gain of 500 V. Each channel corresponded to 7.9 nm. The pinhole was set to 1.25 Airy units at 550 nm emission. Transmitted light (DIC) was registered together with fluorescence. Images were collected in tile-based mode (5 × 5), with total area of 1220 × 1220 μm, 0.13 μm pixel size and 2.05 μs dwell time. All signals were digitized with 16-bit precision.

Microscopy: microplate reader. The cytotoxicity assay plates were imaged (4× magnification) using a Cytation3 microplate reader mounted with 4 filter cubes (BioTek Agilent): DAPI (λ_{ex} 350–405 nm, λ_{em} 415–480 nm), GFP (λ_{ex} 445–490 nm, λ_{em} 501–550 nm), RFP (λ_{ex} 505–560 nm, λ_{em} 520–570 nm) and Texas Red (λ_{ex} 575–600 nm, λ_{em} 510–585 nm). Image analysis and cell counts were performed in the BioTekGen5 software.

UV/VIS-fluorescence spectrophotometer. Cells isolated from *Pocillopora damicornis* (mixed cells: coral host and symbiotic algae) suspended in sterile artificial seawater were analyzed using a Varian Cary Eclipse Fluorimeter with the following settings: scan from λ_{ex} 200–700/ λ_{em} 350–900, excitation slit 20 nm, emission slit 5 nm, scan rate 9600.00 nm/min, data interval 2.00 nm, average time 0.0125 s, auto excitation filter, open emission filter, medium PMT voltage, no corrected spectra. The resulting data was used to produce the excitation–emission matrix presented in Fig. 3.

Data availability

All spectral scans performed on *Pocillopora damicornis* mentioned in the Results section and Supplementary Materials S.1 are available on the Open Science Framework repository <https://osf.io/69jpx/> (<https://doi.org/10.17605/OSF.IO/69JPX>). All *Pocillopora damicornis* protein sequences and human protein sequences analyzed in the Discussion and Supplementary Materials S.3 are available in UniProtKB <https://www.uniprot.org/>. The remainder of the data generated in this study are presented in the text or in Supplementary Materials.

Received: 17 April 2022; Accepted: 31 August 2022

Published online: 12 September 2022

References

- Cummings, B. S. & Schnellmann, R. G. Measurement of cell death in mammalian cells. *Curr. Protoc. Pharmacol.* **25**, 12–18. <https://doi.org/10.1002/0471141755.ph1208s25> (2004).
- Riss, T., Niles, A., Moravec, R., Karassina, N. & Vidugiriene, J. Cytotoxicity assays: In vitro methods to measure dead cells. *Assay Guid. Manual.* <https://www.ncbi.nlm.nih.gov/sites/books/NBK540958/> (2019).
- Lakowicz, J. R. Fluorescence sensing. In *Principles of Fluorescence Spectroscopy* (ed. Lakowicz, J. R.) 623–673 (Springer US, 2006). https://doi.org/10.1007/978-0-387-46312-4_19.
- Roger, L. M. *et al.* Applying model approaches in non-model systems: A review and case study on coral cell culture. *PLoS ONE* **16**, e0248953 (2021).
- Frank, U., Rabinowitz, C. & Rinkevich, B. In vitro establishment of continuous cell cultures and cell lines from ten colonial cnidarians. *Mar. Biol.* **120**, 491–499. <https://doi.org/10.1007/BF00680224> (1994).
- Kawamura, K., Nishitsuji, K., Shoguchi, E., Fujiwara, S. & Satoh, N. Establishing sustainable cell lines of a coral, *Acropora tenuis*. *Mar. Biotechnol.* **23**, 1–16. <https://doi.org/10.1007/s10126-021-10031-w> (2021).
- Nowotny, J. D., Connelly, M. T. & Traylor-Knowles, N. Novel methods to establish whole-body primary cell cultures for the cnidarians *Nematostella vectensis* and *Pocillopora damicornis*. *Sci. Rep.* **11**, 1–9. <https://doi.org/10.1038/s41598-021-83549-7> (2021).
- Awad, D., Schrader, I., Bartok, M., Mohr, A. & Gabel, D. Comparative Toxicology of trypan blue, brilliant blue G, and their combination together with polyethylene glycol on human pigment epithelial cells. *Investig. Ophthalmol. Vis. Sci.* **52**, 4085–4090. <https://doi.org/10.1167/iops.10-6336> (2011).
- Woodley, C. & Downs, C. *Ecological Risk Assessment of Munitions Compounds on Coral and Coral Reef Health* (National Oceanic and Atmospheric Administration Charleston SC Hollings Marine Lab, 2014).
- Woodley, C. M., Downs, C. A., Bruckner, A. W., Porter, J. W. & Galloway, S. B. Chapter 37: Coral cell and tissue culture methods. In *Diseases of Coral* (eds Woodley, C. M. *et al.*) 489–505 (Wiley, 2016).
- Franklin, D. J., Hoegh-Guldberg, O., Jones, R. & Berges, J. A. Cell death and degeneration in the symbiotic dinoflagellates of the coral *Stylophora pistillata* during bleaching. *Mar. Ecol. Prog. Ser.* **272**, 117–130. <https://doi.org/10.3354/meps272117> (2004).
- Franklin, D. J., Cedrés, C. M. M. & Hoegh-Guldberg, O. Increased mortality and photoinhibition in the symbiotic dinoflagellates of the Indo-Pacific coral *Stylophora pistillata* (Esper) after summer bleaching. *Mar. Biol.* **149**, 633–642. <https://doi.org/10.1007/s00227-005-0230-z> (2006).
- Bessette, P. H. & Daugherty, P. S. Flow cytometric screening of cDNA expression libraries for fluorescent proteins. *Biotechnol. Prog.* **20**, 963–967. <https://doi.org/10.1021/bp034308g> (2004).
- Shimomura, O., Johnson, F. H. & Saiga, Y. Extraction, purification and properties of aequorin, a bioluminescent protein from the luminous Hydromedusa, *Aequorea*. *J. Cell. Comp. Physiol.* **59**, 223–239. <https://doi.org/10.1002/jcp.1030590302> (1962).
- Zimmer, M. GFP: From jellyfish to the Nobel prize and beyond. *Chem. Soc. Rev.* **38**, 2823–2832. <https://doi.org/10.1039/B904023D> (2009).
- Alieva, N. O. *et al.* Diversity and evolution of coral fluorescent proteins. *PLoS ONE* **3**, e2680. <https://doi.org/10.1371/journal.pone.0002680> (2008).
- Kelmanson, I. V. & Matz, M. V. Molecular basis and evolutionary origins of color diversity in great star coral *Montastraea cavernosa* (Scleractinia: Faviida). *Mol. Biol. Evol.* **20**, 1125–1133. <https://doi.org/10.1093/molbev/msg130> (2003).

18. Labas, Y. A. *et al.* Diversity and evolution of the green fluorescent protein family. *Proc. Natl. Acad. Sci.* **99**, 4256–4261. <https://doi.org/10.1073/pnas.062552299> (2002).
19. Mazel, C. H. Spectral measurements of fluorescence emission in *Caribbean cnidarians*. *Mar. Ecol. Prog. Ser. Oldendorf* **120**, 185–191. <https://doi.org/10.3354/meps120185> (1995).
20. Bridges, M. C., Woodley, C. M., Peters, E. C., May, L. A. & Galloway, S. B. Expression and characterization of a bright far-red fluorescent protein from the pink-pigmented tissues of *Porites lobata*. *Mar. Biotechnol.* **22**, 67–80. <https://doi.org/10.1007/s10126-019-09931-9> (2020).
21. Huang, K. T., Chen, Y. H. & Walker, A. M. Inaccuracies in MTS assays: Major distorting effects of medium, serum albumin, and fatty acids. *Biotechniques* **37**, 406–412. <https://doi.org/10.21440/04373ST05> (2004).
22. Kumar, P., Nagarajan, A. & Uchil, P. D. Analysis of cell viability by the lactate dehydrogenase assay. *Cold Spring Harbor Protoc.* **2018**, pdb-prot095497. <https://doi.org/10.1101/pdb.prot095497> (2018).
23. Downs, C. A., Fauth, J. E., Downs, V. D. & Ostrander, G. K. In vitro cell-toxicity screening as an alternative animal model for coral toxicology: Effects of heat stress, sulfide, rotenone, cyanide, and cuprous oxide on cell viability and mitochondrial function. *Ecotoxicology* **19**, 171–184. <https://doi.org/10.1007/s10646-009-0403-5> (2010).
24. Riss, T. L. *et al.* Cell viability assays. *Assay Guid. Manual*. <https://www.ncbi.nlm.nih.gov/books/NBK574243/?report=reader> (2016).
25. Linsmayer, L. B., Deheyn, D. D., Tomanek, L. & Tresguerres, M. Dynamic regulation of coral energy metabolism throughout the diel cycle. *Sci. Rep.* **10**, 19881. <https://doi.org/10.1038/s41598-020-76828-2> (2020).
26. Thomas, M. G., Marwood, R. M., Parsons, A. E. & Parsons, R. B. The effect of foetal bovine serum supplementation upon the lactate dehydrogenase cytotoxicity assay: Important considerations for in vitro toxicity analysis. *Toxicol. In Vitro* **30**, 300–308. <https://doi.org/10.1016/j.tvi.2015.10.007> (2015).
27. Li, S., Wallis, L. K., Ma, H. & Diamond, S. A. Phototoxicity of TiO₂ nanoparticles to a freshwater benthic amphipod: Are benthic systems at risk? *Sci. Total Environ.* **466–467**, 800–808. <https://doi.org/10.1016/j.scitotenv.2013.07.059> (2014).
28. Menard, A., Drobne, D. & Jemec, A. Ecotoxicity of nanosized TiO₂. Review of in vivo data. *Environ. Pollut.* **159**, 677–684. <https://doi.org/10.1016/j.envpol.2010.11.027> (2011).
29. Minetto, D., Libralato, G. & Volpi Ghirardini, A. Ecotoxicity of engineered TiO₂ nanoparticles to saltwater organisms: An overview. *Environ. Int.* **66**, 18–27. <https://doi.org/10.1016/j.envint.2014.01.012> (2014).
30. Corimaldesi, C., Marcellini, F., Nepote, E., Damiani, E. & Danovaro, R. Impact of inorganic UV filters contained in sunscreen products on tropical stony corals (*Acropora* spp.). *Sci. Total Environ.* **637–638**, 1279–1285. <https://doi.org/10.1016/j.scitotenv.2018.05.108> (2018).
31. Jovanović, B. & Guzmán, H. M. Effects of titanium dioxide (TiO₂) nanoparticles on Caribbean reef-building coral (*Montastraea faveolata*). *Environ. Toxicol. Chem.* **33**, 1346–1353. <https://doi.org/10.1002/etc.2560> (2014).
32. Labille, J. *et al.* Assessing UV filter inputs into beach waters during recreational activity: A field study of three French Mediterranean beaches from consumer survey to water analysis. *Sci. Total Environ.* **706**, 136010. <https://doi.org/10.1016/j.scitotenv.2019.136010> (2020).
33. Tovar-Sánchez, A. *et al.* Sunscreen products as emerging pollutants to coastal waters. *PLoS ONE* **8**(6), e65451. <https://doi.org/10.1371/journal.pone.0065451> (2013).
34. Muthukumar, G. & Lenard, J. A preproinsulin-like pseudogene from *Neurospora crassa*. *Mol. Cell. Endocrinol.* **82**, 275–283. [https://doi.org/10.1016/0303-7207\(91\)90041-P](https://doi.org/10.1016/0303-7207(91)90041-P) (1991).
35. Baig, A. M. & Khaleeq, A. First reports of effects of insulin, human-like insulin receptors and adapter proteins in *Acanthamoeba castellanii*. *Sci. Rep.* **10**, 1–14. <https://doi.org/10.1038/s41598-020-63435-4> (2020).
36. Remmert, M., Biegert, A., Hauser, A. & Söding, J. HHblits: Lightning-fast iterative protein sequence searching by HMM–HMM alignment. *Nat. Methods* **9**, 173–175. <https://doi.org/10.1038/nmeth.1818> (2012).
37. Murthy, M. H. S. *et al.* Insulin signaling and pharmacology in corals. *Drug Discov. Today* (under review) (2022).
38. Rege, N. K. *et al.* “Register-shift” insulin analogs uncover constraints of proteotoxicity in protein evolution. *J. Biol. Chem.* **295**, 3080–3098. <https://doi.org/10.1074/jbc.RA119.011389> (2020).
39. Liu, M. *et al.* Biosynthesis, structure, and folding of the insulin precursor protein. *Diabetes Obes. Metab.* **20**, 28–50. <https://doi.org/10.1111/dom.13378> (2018).
40. Weiss, M. A. & Lawrence, M. C. A thing of beauty: Structure and function of insulin’s “aromatic triplet”. *Diabetes Obes. Metab.* **20**, 51–63. <https://doi.org/10.1111/dom.13402> (2018).
41. Grudzielanek, S. *et al.* Cytotoxicity of insulin within its self-assembly and amyloidogenic pathways. *J. Mol. Biol.* **370**, 372–384. <https://doi.org/10.1016/j.jmb.2007.04.053> (2007).
42. Chatani, E., Imamura, H., Yamamoto, N. & Kato, M. Stepwise organization of the β-structure identifies key regions essential for the propagation and cytotoxicity of insulin amyloid fibrils. *J. Biol. Chem.* **289**, 10399–10410. <https://doi.org/10.1074/jbc.M113.520874> (2014).
43. Dayeh, V. R., Chow, S. L., Schirmer, K., Lynn, D. H. & Bols, N. C. Evaluating the toxicity of Triton X-100 to protozoan, fish, and mammalian cells using fluorescent dyes as indicators of cell viability. *Ecotoxicol. Environ. Saf.* **57**, 375–382. [https://doi.org/10.1016/S0147-6513\(03\)00083-6](https://doi.org/10.1016/S0147-6513(03)00083-6) (2004).
44. Krysko, D. V., Vanden Berghe, T., D’Herde, K. & Vandenabeele, P. Apoptosis and necrosis: Detection, discrimination and phagocytosis. *Methods* **44**, 205–221. <https://doi.org/10.1016/j.ymet.2007.12.001> (2008).
45. Oakley, C. A. & Davy, S. K. Cell biology of coral bleaching. In *Coral Bleaching: Ecological Studies* Vol. 233 (eds van Oppen, M. & Lough, J.) (Springer, 2018). https://doi.org/10.1007/978-3-319-75393-5_8.
46. Klenow, M. B., Heitmann, A. S. B., Nylandsted, J. & Simonsen, A. C. Timescale of hole closure during plasma membrane repair estimated by calcium imaging and numerical modeling. *Sci. Rep.* **11**, 4226. <https://doi.org/10.1038/s41598-021-82926-6> (2021).
47. Yavin, E. & Yavin, Z. Attachment and culture of dissociated cells from rat embryo cerebral hemispheres on polylysine-coated surface. *J. Cell Biol.* **62**, 540. <https://doi.org/10.1083/jcb.62.2.540> (1974).
48. Hlina, B. L., Birceanu, O., Robinson, C. S., Dhiyebi, H. & Wilkie, M. P. The relationship between thermal physiology and lampricide sensitivity in larval sea lamprey (*Petromyzon marinus*). *J. Great Lakes Res.* **47**, S272–S284. <https://doi.org/10.1016/j.jglr.2021.10.002> (2021).
49. Dove, S., Hoegh-Guldberg, O. & Ranganathan, S. Major colour patterns of reef-building corals are due to a family of GFP-like proteins. *Coral Reefs* **19**, 197–204. <https://doi.org/10.1007/PL00006956> (2001).
50. Schlichter, D., Fricke, H. & Weber, W. Light harvesting by wavelength transformation in a symbiotic coral of the Red Sea twilight zone. *Mar. Biol.* **91**, 403–407. <https://doi.org/10.1007/BF00428634> (1986).
51. Papina, M., Sakihama, Y., Bena, C., Van Woesik, R. & Yamasaki, H. Separation of highly fluorescent proteins by SDS-PAGE in Acroporidae corals. *Comp. Biochem. Physiol. B Biochem. Mol. Biol.* **131**, 767–774. [https://doi.org/10.1016/S1096-4959\(02\)00025-8](https://doi.org/10.1016/S1096-4959(02)00025-8) (2002).
52. Salih, A. *et al.* Biological properties of coral GFP-type proteins provide clues for engineering novel optical probes and biosensors. In *Genetically Engineered and Optical Probes for Biomedical Applications II*, Vol. 5329, 61–72 (SPIE, 2004). <https://doi.org/10.1117/12.548926>.
53. Salih, A., Larkum, A., Cox, G., Kühl, M. & Hoegh-Guldberg, O. Fluorescent pigments in corals are photoprotective. *Nature* **408**, 850–853. <https://doi.org/10.1038/35048564> (2000).

54. Lesser, M. P. Depth-dependent photoacclimatization to solar ultraviolet radiation in the Caribbean coral *Montastraea faveolata*. *Mar. Ecol. Prog. Ser.* **192**, 137–151. <https://doi.org/10.3354/meps192137> (2000).
55. Fuchs, E. *Fluorescence in Reef Corals (Doctoral Dissertation)* (Massachusetts Institute of Technology, 1999). <http://hdl.handle.net/1721.1/8966>.
56. Cox, G. & Salih, A. Fluorescence lifetime imaging of coral fluorescent proteins. *Microsc. Microanal.* **11**, 256–257. <https://doi.org/10.1017/S143192760551016X> (2005).
57. Lapshin, G. *et al.* Fluorescence color diversity of great barrier reef corals. *J. Innov. Opt. Health Sci.* **8**, 1550028. <https://doi.org/10.1142/S1793545815500285> (2015).
58. Karasawa, S., Araki, T., Yamamoto-Hino, M. & Miyawaki, A. A green-emitting fluorescent protein from Galaxeidae coral and its monomeric version for use in fluorescent labeling. *J. Biol. Chem.* **278**, 34167–34171. <https://doi.org/10.1074/jbc.M304063200> (2003).
59. Apprill, A. M. & Lesser, M. P. Effects of ultraviolet radiation on *Laminaria saccharina* in relation to depth and tidal height in the Gulf of Maine. *Mar. Ecol. Prog. Ser.* **256**, 75–85. <https://doi.org/10.3354/meps256075> (2003).
60. Mazel, C. H. *et al.* Green-fluorescent proteins in Caribbean corals. *Limnol. Oceanogr.* **48**, 402–411. https://doi.org/10.4319/lo.2003.48.1_part_2.0402 (2003).
61. Pedrós, R., Moya, I., Goulas, Y. & Jacquemoud, S. Chlorophyll fluorescence emission spectrum inside a leaf. *Photochem. Photobiol. Sci.* **7**, 498–502. <https://doi.org/10.1039/b719506k> (2008).

Acknowledgements

The authors would like to thank all contributors to the Synthetic Coral Harnessing the Data Revolution project. We also thank Nicholas Rodriguez for his assistance with implementing the R ecotox package. This material is based upon work supported by the National Science Foundation under NSF Award Number 1939699. Services in support of the research project were generated by the VCU Massey Cancer Center Health Communication and Digital Innovation Shared Resource core, Microscopy Core shared resource, supported, in part, with funding from NIH-NCI Cancer Center Support Grant P30 CA016059.

Author contributions

Conceptualization: L.M.R., N.A.L.; data curation: L.M.R., Y.A.D., M.O.; formal analysis: L.M.R.; funding acquisition: N.A.L., T.B., J.K.S., L.C.; investigation: L.M.R., Y.A.D.; methodology: L.M.R., N.A.L.; project administration: L.M.R.; resources: N.A.L., T.B., F.W.; supervision: N.A.L., T.B., F.W., L.C.; validation: L.M.R.; visualization: L.M.R., N.A.L., T.B., F.W., M.O.; writing—original draft: L.M.R., N.A.L., T.B., F.W., Y.A.D., J.K.S.; writing—review and editing: L.M.R., N.A.L., T.B., F.W., J.K.S., L.C.

Competing interests

The authors declare no competing interests.

Additional information

Supplementary Information The online version contains supplementary material available at <https://doi.org/10.1038/s41598-022-19586-7>.

Correspondence and requests for materials should be addressed to L.M.R. or N.A.L.

Reprints and permissions information is available at www.nature.com/reprints.

Publisher's note Springer Nature remains neutral with regard to jurisdictional claims in published maps and institutional affiliations.



Open Access This article is licensed under a Creative Commons Attribution 4.0 International License, which permits use, sharing, adaptation, distribution and reproduction in any medium or format, as long as you give appropriate credit to the original author(s) and the source, provide a link to the Creative Commons licence, and indicate if changes were made. The images or other third party material in this article are included in the article's Creative Commons licence, unless indicated otherwise in a credit line to the material. If material is not included in the article's Creative Commons licence and your intended use is not permitted by statutory regulation or exceeds the permitted use, you will need to obtain permission directly from the copyright holder. To view a copy of this licence, visit <http://creativecommons.org/licenses/by/4.0/>.

© The Author(s) 2022